CHIN. PHYS. LETT. Vol. 34, No. 7 (2017) 075201

Linear Growth of Rayleigh–Taylor Instability of Two Finite-Thickness Fluid Layers *

Hong-Yu Guo(郭宏宇)[1,2], Li-Feng Wang(王立锋)[2,3], Wen-Hua Ye(叶文华)[2,3]**, Jun-Feng Wu(吴俊峰)[2], Wei-Yan Zhang(张维岩)[2]

[1]*Graduate School, China Academy of Engineering Physics, Beijing 100088*
[2]*Institute of Applied Physics and Computational Mathematics, Beijing 100094*
[3]*HEDPS, Center for Applied Physics and Technology, Peking University, Beijing 100871*

(Received 12 January 2017)

The linear growth of Rayleigh–Taylor instability (RTI) of two superimposed finite-thickness fluids in a gravitational field is investigated analytically. Coupling evolution equations for perturbation on the upper, middle and lower interfaces of the two stratified fluids are derived. The growth rate of the RTI and the evolution of the amplitudes of perturbation on the three interfaces are obtained by solving the coupling equations. It is found that the finite-thickness fluids reduce the growth rate of perturbation on the middle interface. However, the finite-thickness effect plays an important role in perturbation growth even for the thin layers which will cause more severe RTI growth. Finally, the dependence of the interface position under different initial conditions are discussed in some detail.

PACS: 52.57.Fg, 47.20.Ma, 52.35.Py DOI: 10.1088/0256-307X/34/7/075201

The Rayleigh–Taylor instability (RTI)[1,2] occurs when a light fluid supports a heavy fluid in a gravitational field or a lighter fluid accelerates a heavier one. RTI plays a vital role in successful inertial confinement fusion (ICF)[3] and astrophysics.[4] In typical accelerated ICF capsules, RTI is the major problem restricting the achievement of high compression and symmetry.[5] Therefore, RTI growth must be limited to an acceptable level in ICF implosion experiments.

The classical RTI growth case[1,2] is a semi-infinite fluid of constant density ρ_1 accelerating a semi-infinite fluid of density ρ_2 ($\rho_2 > \rho_1$) with acceleration g. Small perturbation on the interface will grow exponentially in time with the linear growth rate $\gamma = \sqrt{Akg}$, where $k = 2\pi/\lambda$ is the wave number, λ is the wavelength of initial perturbation, and $A = (\rho_2 - \rho_1)/(\rho_2 + \rho_1)$ is the Atwood number. Much work has been carried out to deal with the configuration of this semi-infinite fluids that take different effects into consideration.[6–11] The typical ICF implosion capsule contains two layers, a finite fuel layer on the inside and an ablator layer distributing outside. Therefore, there exist at least three interfaces, which are hot-spot boundary, fuel-ablator interface and ablator front, respectively. Studying the RTI growth of perturbation at the three interfaces and the effect of the finite-thickness on the RTI growth is of great significance. Taylor[2] first explored a model where a fluid layer is accelerated by uniform pressure. Recently, a weakly nonlinear model[12] has been established to study the nonlinear RTI growth of a single thin shell. The linear growth rate of RTI at the $N-1$ interfaces of arbitrary N superimposed fluids has been discussed by Mikaelian.[13–15] However, only the case $N = 3$ with two interfaces is obtained analytically. For $N > 3$, a numerical method was introduced to calculate an eigenvalue problem. In this study, RTI growth of the case $N = 4$ (the first and the last layers are vacuum) with three interfaces is investigated analytically in a different way. The potential theory used here can be extended to investigate the nonlinear RTI[12] growth of multi-layer fluid which will be pursued in the following research.

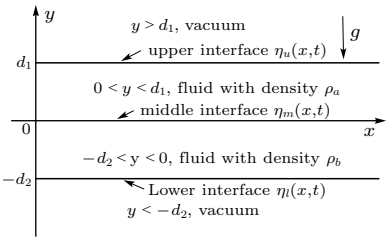

Fig. 1. Schematic drawing of two finite-thickness fluid layers considered in this study.

We consider two incompressible, inviscid and irrotational fluids immersing in a gravitational field $-g\boldsymbol{e}_y$ as shown in Fig. 1. The fluid of density ρ_a lies above with thickness d_1 and the fluid below of density ρ_b with thickness d_2. A Cartesian coordinate system is established, where x and y are along and normal to the unperturbed interface, respectively. The regions $y > d_1$ and $y < -d_2$ are vacuum. The physical quantities on the upper, middle and lower interface shall be denoted by subscripts 1, 2 and 3, respectively. The physical quantities of fluid above are denoted by subscript a and that below by b.

At the middle interface, the normal velocity is continuous across the interface. At the upper and lower interfaces, the normal velocities are zero for free

*Supported by the National Natural Science Foundation of China under Grant Nos 11275031, 11475034, 11575033 and 11274026, and the National Basic Research Program of China under Grant No 2013CB834100.
**Corresponding author. Email: ye_wenhua@iapcm.ac.cn
© 2017 Chinese Physical Society and IOP Publishing Ltd

boundary. Therefore, the kinematic boundary conditions are

$$\frac{\partial\eta_{\rm m}}{\partial t}+\frac{\partial\eta_{\rm m}}{\partial x}\frac{\partial\phi_{\rm a}}{\partial x}-\frac{\partial\phi_{\rm a}}{\partial y}=0,\ \text{at}\ y=\eta_{\rm m}, \tag{1}$$

$$\frac{\partial\eta_{\rm m}}{\partial t}+\frac{\partial\eta_{\rm m}}{\partial x}\frac{\partial\phi_{\rm b}}{\partial x}-\frac{\partial\phi_{\rm b}}{\partial y}=0,\ \text{at}\ y=\eta_{\rm m}, \tag{2}$$

$$\frac{\partial\eta_{\rm u}}{\partial t}+\frac{\partial\eta_{\rm u}}{\partial x}\frac{\partial\phi_{\rm a}}{\partial x}-\frac{\partial\phi_{\rm a}}{\partial y}=0,\ \text{at}\ y=d_1+\eta_{\rm u}, \tag{3}$$

$$\frac{\partial\eta_{l}}{\partial t}+\frac{\partial\eta_{l}}{\partial x}\frac{\partial\phi_{\rm b}}{\partial x}-\frac{\partial\phi_{\rm b}}{\partial y}=0,\ \text{at}\ y=-d_2+\eta_{l}, \tag{4}$$

where $\phi_{\rm a}$ and $\phi_{\rm b}$ are velocity potentials, $\eta_{\rm u}$, $\eta_{\rm m}$ and η_l are small perturbations at the three interfaces, which can be expressed as

$$\eta_{\rm u}(x,t)=\eta_1(t)\cos(kx), \tag{5}$$

$$\eta_{\rm m}(x,t)=\eta_2(t)\cos(kx), \tag{6}$$

$$\eta_{l}(x,t)=\eta_3(t)\cos(kx). \tag{7}$$

The velocity potentials describing the incompressible perturbed fluids can be written as

$$\phi_i(x,y,t)=\phi_i^{(0)}(t)+\varphi_i(x,y,t), \tag{8}$$

where $\phi_i^{(0)}(t)$ are the initial unperturbed velocity potentials of the two fluids, and $\varphi_i(x,y,t)$ are the additional perturbed velocity potentials and $\nabla^2\varphi_i=0$ with i denoting a or b. The perturbed velocity potentials obtained by solving the Laplace equation are

$$\varphi_{\rm a}(x,y,t)=[a_1(t)e^{ky}+a_2(t)e^{-ky}]\cos(kx), \tag{9}$$

$$\varphi_{\rm b}(x,y,t)=[b_1(t)e^{ky}+b_2(t)e^{-ky}]\cos(kx), \tag{10}$$

where $a_i(t)$ and $b_i(t)$ are amplitudes of velocity potentials. The Bernoulli equation can be written as

$$p_i=-\rho_i\Big[\frac{\partial\phi_i}{\partial t}+\frac{1}{2}(\nabla\phi_i)^2+gy\Big]+f_i(t), \tag{11}$$

where i=a and b, and $f_i(t)$ is an arbitrary function of time.

Note that the pressure equilibrium conditions $p_{\rm b}^{(0)}|_{y=-d_2}-p_{\rm a}^{(0)}|_{y=d_1}=\rho_{\rm a}d_1g+\rho_{\rm b}d_2g$ at the upper and lower interfaces have been satisfied. Thus the perturbed pressure is zero at the upper and lower interfaces and the pressure at the middle interface is continuous, i.e.,

$$\rho_{\rm a}\Big[\frac{\partial\varphi_{\rm a}}{\partial t}+\frac{1}{2}(\nabla\varphi_{\rm a})^2+g\eta_{\rm u}\Big]=0,\ \text{at}\ y=d_1+\eta_{\rm u}, \tag{12}$$

$$\rho_{\rm b}\Big[\frac{\partial\varphi_{\rm b}}{\partial t}+\frac{1}{2}(\nabla\varphi_{\rm b})^2+g\eta_{l}\Big]=0,\ \text{at}\ y=-d_2+\eta_{l}, \tag{13}$$

$$p_{\rm a}-p_{\rm b}=0,\ \text{at}\ y=\eta_{\rm m}. \tag{14}$$

Inserting Eqs. (5)–(11) into Eqs. (1)–(4) and (12)–(14), seven time-dependent only equations for $\eta_1(t)$, $\eta_2(t)$, $\eta_3(t)$, $a_1(t)$, $a_2(t)$, $b_1(t)$ and $b_2(t)$ are obtained. Eliminating the variables $a_1(t)$, $a_2(t)$, $b_1(t)$ and $b_2(t)$, the coupled second-order ordinary differential equations (ODEs) for $\eta_1(t)$, $\eta_2(t)$ and $\eta_3(t)$ are derived as

$$\frac{d^2\eta_1}{dt^2}-\frac{2e^{-\xi_1}}{1+e^{-2\xi_1}}\frac{d^2\eta_2}{dt^2}+kg\frac{1-e^{-2\xi_1}}{1+e^{-2\xi_1}}\eta_1=0, \tag{15}$$

$$\begin{aligned}&\frac{d^2\eta_2}{dt^2}-\frac{e^{-\xi_1}(1-e^{-2\xi_2})(1+A)}{1-e^{-2(\xi_1+\xi_2)}+(e^{-2\xi_1}-e^{-2\xi_2})A}\frac{d^2\eta_1}{dt^2}\\&-\frac{e^{-\xi_2}(1-e^{-2\xi_1})(1-A)}{1-e^{-2(\xi_1+\xi_2)}+(e^{-2\xi_1}-e^{-2\xi_2})A}\frac{d^2\eta_3}{dt^2}\\&-\frac{(1-e^{-2\xi_1})(1-e^{-2\xi_2})Akg}{1-e^{-2(\xi_1+\xi_2)}+(e^{-2\xi_1}-e^{-2\xi_2})A}\eta_2=0,\end{aligned} \tag{16}$$

$$\frac{d^2\eta_3}{dt^2}-\frac{2e^{-\xi_2}}{1+e^{-2\xi_2}}\frac{d^2\eta_2}{dt^2}-kg\frac{1-e^{-2\xi_2}}{1+e^{-2\xi_2}}\eta_3=0, \tag{17}$$

where $\xi_1=kd_1$ and $\xi_2=kd_2$ are the normalized fluid thicknesses, and $A=(\rho_{\rm a}-\rho_{\rm b})/(\rho_{\rm a}+\rho_{\rm b})$ is the Atwood number. Adopting the most common initial conditions

$$\eta_i(t=0)=\epsilon_i,\ d\eta_i(t=0)/dt=0, \tag{18}$$

where $i=1$, 2 and 3 denotes the initial perturbation at the three interfaces, respectively. With the above initial conditions, the coupling ODEs are solved as

$$\begin{aligned}\eta_1(t)=\frac{1}{\Xi}\{&[(1-\alpha_{23}\alpha_{32})\epsilon_1-\alpha_{21}(\epsilon_2-\alpha_{32}\epsilon_3)\\&-\alpha_{31}(\epsilon_3-\alpha_{23}\epsilon_2)]\cos(\sqrt{kg}t)\\&+\alpha_{21}[(1-\alpha_{13}\alpha_{31})\epsilon_2-\alpha_{12}(\epsilon_1-\alpha_{31}\epsilon_3)\\&-\alpha_{32}(\epsilon_3-\alpha_{13}\epsilon_1)]\cosh(\gamma t)\\&+\alpha_{31}[(1-\alpha_{12}\alpha_{21})\epsilon_3-\alpha_{13}(\epsilon_1-\alpha_{21}\epsilon_2)\\&-\alpha_{23}(\epsilon_2-\alpha_{12}\epsilon_1)]\cosh(\sqrt{kg}t)\},\end{aligned} \tag{19}$$

$$\begin{aligned}\eta_2(t)=\frac{1}{\Xi}\{&[(1-\alpha_{13}\alpha_{31})\epsilon_2-\alpha_{12}(\epsilon_1-\alpha_{31}\epsilon_3)\\&-\alpha_{32}(\epsilon_3-\alpha_{13}\epsilon_1)]\cosh(\gamma t)\\&+\alpha_{12}[(1-\alpha_{23}\alpha_{32})\epsilon_1-\alpha_{21}(\epsilon_2-\alpha_{32}\epsilon_3)\\&-\alpha_{31}(\epsilon_3-\alpha_{23}\epsilon_2)]\cos(\sqrt{kg}t)\\&+\alpha_{32}[(1-\alpha_{12}\alpha_{21})\epsilon_3-\alpha_{13}(\epsilon_1-\alpha_{21}\epsilon_2)\\&-\alpha_{23}(\epsilon_2-\alpha_{12}\epsilon_1)]\cosh(\sqrt{kg}t)\},\end{aligned} \tag{20}$$

$$\begin{aligned}\eta_3(t)=\frac{1}{\Xi}\{&[(1-\alpha_{12}\alpha_{21})\epsilon_3-\alpha_{13}(\epsilon_1-\alpha_{21}\epsilon_2)\\&-\alpha_{23}(\epsilon_2-\alpha_{12}\epsilon_1)]\cosh(\sqrt{kg}t)\\&+\alpha_{23}[(1-\alpha_{13}\alpha_{31})\epsilon_2-\alpha_{12}(\epsilon_1-\alpha_{31}\epsilon_3)\\&-\alpha_{32}(\epsilon_3-\alpha_{13}\epsilon_1)]\cosh(\gamma t)\\&+\alpha_{13}[(1-\alpha_{23}\alpha_{32})\epsilon_1-\alpha_{21}(\epsilon_2-\alpha_{32}\epsilon_3)\\&-\alpha_{31}(\epsilon_3-\alpha_{23}\epsilon_2)]\cos(\sqrt{kg}t)\},\end{aligned} \tag{21}$$

where $\Xi=1-\alpha_{12}\alpha_{21}-\alpha_{13}\alpha_{31}-\alpha_{23}\alpha_{32}+\alpha_{12}\alpha_{23}\alpha_{31}+\alpha_{13}\alpha_{21}\alpha_{32}$, and the perturbation feedthrough coeffi-

cients α_{12}, α_{13}, α_{21}, α_{23}, α_{31} and α_{32} are

$$\alpha_{12} = e^{-\xi_1}, \alpha_{32} = e^{-\xi_2}, \tag{22}$$

$$\alpha_{13} = \alpha_{31} = e^{-\xi_1-\xi_2}, \tag{23}$$

$$\alpha_{21} = \frac{2e^{-\xi_1}(1-e^{-2\xi_2})}{1-e^{-2(\xi_1+\xi_2)}}\frac{A}{1+A}, \tag{24}$$

$$\alpha_{23} = -\frac{2e^{-\xi_2}(1-e^{-2\xi_1})}{1-e^{-2(\xi_1+\xi_2)}}\frac{A}{1-A}, \tag{25}$$

where the coefficients α_{ij} ($i = 1$, 2 and 3, $j = 1$, 2 and 3, and $i \neq j$) denote the perturbation feedthrough factor from interface i to interface j, respectively. When $\xi_1 \to \infty$ and $\xi_2 \to \infty$, Eq. (20) is reduced to the classical result of RTI growth.[16]

As can be seen from linear solutions (19)–(21), the three interfaces are coupled, especially when $\xi_1 < 1$ and $\xi_2 < 1$. The upper interface is stable initially with perturbation frequency $i\sqrt{kg}$, and the lower interface is unstable with growth rate $\sqrt{kg}$, which is not affected by the fluid thickness. The growth rate γ at the middle interface is

$$\gamma = \sqrt{\frac{(1-e^{-2\xi_1})(1-e^{-2\xi_2})Akg}{1-e^{-2(\xi_1+\xi_2)}-(e^{-2\xi_1}-e^{-2\xi_2})A}}, \tag{26}$$

where the explicit fluid thickness ξ_1, ξ_2 and the Atwood number A dependencies of the γ are displayed clearly. When the upper fluid thickness ξ_1 is finite, in the limit of $\xi_2 \to \infty$, the growth rate takes the form

$$\gamma(\xi_2 \to \infty) = \sqrt{Akg\frac{1-e^{-2\xi_1}}{1-e^{-2\xi_1}A}}, \tag{27}$$

which is identical to the result of Goncharov.[17] When both the fluids are infinity, the growth rate is

$$\gamma(\xi_1 \to \infty, \xi_2 \to \infty) = \sqrt{Akg}, \tag{28}$$

which is the classical result.[16]

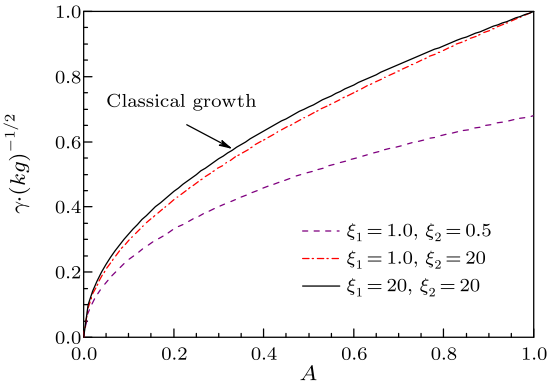

Fig. 2. The normalized growth rate $\gamma/\sqrt{kg}$ of the middle interface versus the Atwood number A for different fluid thicknesses. Here $\xi_1 = 1.0$, $\xi_2 = 20$ (dotted-dashed line) represents a finite fluid is atop an infinity fluid, and $\xi_1 = 1.0$, $\xi_2 = 0.5$ (dashed line) indicates that both the fluids are finite. The classical growth rate is $\xi_1 = \xi_2 = 20$ (solid line).

The normalized growth rate $\gamma/\sqrt{kg}$ of the perturbation at the middle interface versus the Atwood number A for different fluid thicknesses ξ_1 and ξ_2 is given in Fig. 2. For a fixed Atwood number A, finite fluid thicknesses ξ_1 and ξ_2 will reduce the growth rate of perturbation. The largest reduction will only be for the long wavelength perturbation ($\xi_i < 1$). However, long wavelength perturbation will lead to more serious RTI growth, which will be shown in the following.

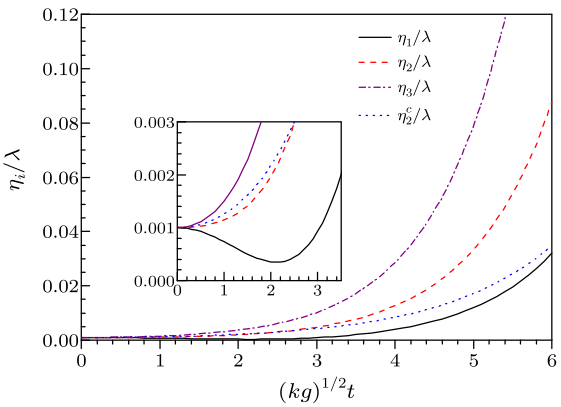

Fig. 3. The evolution of the amplitude of perturbation η_1/λ (solid line), η_2/λ (dashed line) and η_3/λ (dot-dashed line) for $A = 0.5$ with initial perturbation amplitudes $\epsilon_1 = \epsilon_2 = \epsilon_3 = 0.001\lambda$. The two fluid thicknesses are $\xi_1 = \xi_2 = 1.0$. The classical result η_2^c/λ (dotted line) with $\xi_1 = \xi_2 = \infty$ is plotted for comparison.

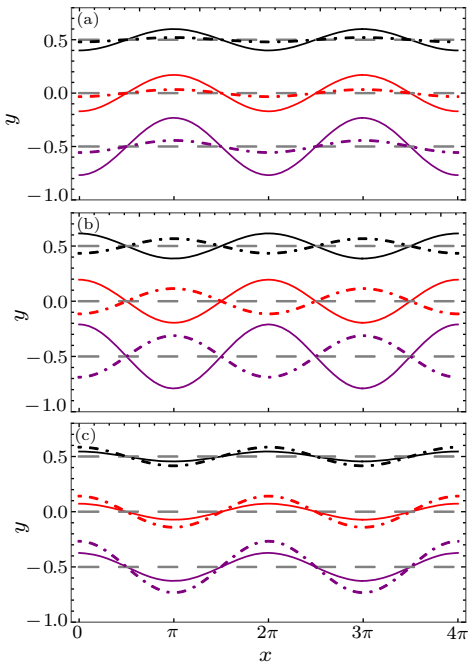

Fig. 4. The position of the upper, middle and lower interfaces initiated by only the upper interface perturbation (a), only the middle interface perturbation (b) and only the lower interface perturbation (c) for $A = 0.5$ (solid line), -0.5 (dash-dotted line) at $\sqrt{kg}t = 5.8$, respectively. The two fluid thicknesses are $\xi_1 = \xi_2 = 0.5$.

In Fig. 3, we plot the evolution of normalized amplitudes of perturbation $\eta_i/\lambda (i = 1, 2, 3)$ on the upper, middle and lower interfaces, respectively. The classical

growth of perturbation η_2^c/λ is also contained for comparison. The initial displacement amplitudes at three interfaces are $\epsilon_1 = \epsilon_2 = \epsilon_3 = 0.001\lambda$. The fluid thicknesses are $\xi_1 = \xi_2 = 1.0$. Note that the amplitude of upper interface η_1/λ oscillates in the beginning as the upper interface is stable initially, then the amplitude begins to increase with time $\sqrt{kg}t$ because of the feedback effects from the middle and lower interfaces and the upper interface becomes unstable. The perturbation amplitude η_2/λ at the middle interface is less than the classical linear growth of amplitude η_2^c/λ at the early time because the growth rate γ of the finite-thickness fluid is less than the classical growth rate $\sqrt{kg}$. At later times, the perturbation amplitude η_2/λ is greater than η_2^c/λ as the feedback effects from upper and lower interfaces become important. The perturbation amplitude η_3/λ at the lower interface grows faster than the classical amplitude η_2^c/λ as the lower interface is unstable at the beginning with growth rate $\sqrt{kg}$ and the perturbation amplitude η_3/λ grows even more rapidly because of the coupling effects from the upper and middle interfaces.

The dependence of the interface positions on the different initial conditions are illustrated in Fig. 4 for fixed fluid thicknesses $\xi_1 = \xi_2 = 0.5$ at normalized time $\sqrt{kg}t = 5.8$. The Atwood number $A = 0.5$ is described with solid and dashed lines for $A = -0.5$. In Fig. 4(a), we only impose a perturbation on the upper interface and the other two interfaces are kept unperturbed initially, namely, $\epsilon_1 = 0.001\lambda$, $\epsilon_2 = \epsilon_3 = 0$. The phases of three interfaces are shifted by π in comparison to the initially cosinusoidal perturbation. This is because the perturbation of upper interface feeds through to the middle interface with initial amplitude $-(\alpha_{12} - \alpha_{13}\alpha_{32})\epsilon_1 < 0$ and couples to the lower interface with the amplitude $-(\alpha_{13} - \alpha_{12}\alpha_{23})\epsilon_1 < 0$. It is clear that the negative feedback will lead to phase inversion on the middle and lower interfaces. As the RTI growth is initiated on the middle and lower interfaces, the perturbations will feed through to the upper interface and the perturbation phase of the three interfaces will be the same finally. In Fig. 4(b), only the middle interface is perturbed initially with $\epsilon_2 = 0.001\lambda$, $\epsilon_1 = \epsilon_3 = 0$. When $A = 0.5 > 0$, the phases of the perturbation on the three interfaces are the same as the initial perturbation. However for $A = -0.5 < 0$, the phases of perturbation are all changed by π. When $A < 0$ and $\alpha_{23} > 0$, the feedback effect from the middle interface to the lower interface is negative, which will result in shifting of phase. As the perturbation on the lower interface grows faster, perturbation couples to the other two interfaces and the perturbation phases are all changed by π. When $A > 0$, the perturbation of the three interfaces are the same as the initial perturbation as the feedback effect is positive. In Fig. 4(c), only the lower interface is initially imposed with a small perturbation with $\epsilon_3 = 0.001\lambda$, $\epsilon_1 = \epsilon_2 = 0$. As can be seen, $A = -0.5$ will lead to more severe RTI growth than $A = 0.5$. This is because when $A > 0$ and $\alpha_{23} < 0$ the perturbation feeds back from the middle interface to the lower interface and reduces the linear growth of the lower interface, which can be seen in Eq. (21). As the coupling effects from the lower interface to the other two interfaces are positive, thus the perturbation growth on the upper and middle interfaces is consistent with that of the lower interface when only the lower interface is initiated by a small perturbation. This phenomenon can be roughly observed, as the perturbation growth at three interfaces are required by mass conservation.

In conclusion, for two ideal incompressible finite-thickness fluids, the coupling evolution equations for RTI growth on the upper, middle and lower interfaces are derived. The growth rate and the evolution of the amplitudes of perturbation are obtained analytically. It is found that the growth rate γ of the middle interface is reduced by the finite fluids. However, for finite-thickness fluids, the feedthrough effect among the interfaces becomes important especially for $\xi_i < 1$, which will cause more severe RTI growth. The dependence of interface position on the initial condition is discussed. The explicit dependence of feedback effect on the initial perturbation and the Atwood number A at the interface are displayed clearly. Thus it should be considered in application where the feedthrough effect is very important, such as ICF implosions.

References

[1] Rayleigh L 1883 *Proc. London Math. Soc.* **14** 170
[2] Taylor G 1950 *Proc. R. Soc. London Ser.* A **201** 192
[3] Atzeni S et al 2004 *The Physics of Inertial Fusion: Beam Plasma Interaction Hydrodynamics, Hot Dense Mater* (Oxford University)
[4] Remington B A, Drake R P and Ryutov D D 2006 *Rev. Mod. Phys.* **78** 755
[5] Lindl J D et al 2004 *Phys. Plasmas* **11** 339
[6] Ye W H, Zhang W Y and He X T 2002 *Phys. Rev.* E **65** 057401
[7] Guo H Y et al 2014 *Chin. Phys. Lett.* **31** 044702
[8] Wang L F, Wu J F, Guo H Y, Ye W H, Liu J, Zhang W Y and He X T 2015 *Phys. Plasmas* **22** 082702
[9] Jacobs J W and Catton I 1988 *J. Fluid Mech.* **187** 329
[10] Ye W H, Wang L F and He X T 2010 *Phys. Plasmas* **17** 122704
[11] Liu W H, Wang L F, Ye W H and He X T 2012 *Phys. Plasmas* **19** 042705
[12] Wang L F, Guo H Y, Wu J F, Ye W H, Liu J, Zhang W Y and He X T 2014 *Phys. Plasmas* **21** 122710
[13] Mikaelian K O 1982 *Phys. Rev. Lett.* **48** 1365
[14] Mikaelian K O 1982 *Phys. Rev.* A **26** 2140
[15] Mikaelian K O 1983 *Phys. Rev.* A **28** 1637
[16] Wang L F, Ye W H and Li Y J 2010 *Chin. Phys. Lett.* **27** 025203
[17] Goncharov V N et al 2000 *Phys. Plasmas* **7** 5118